J Neurophysiol 94: 2019–2030, 2005.
First published May 31, 2005; doi:10.1152/jn.00860.2004.

Auditory Thalamocortical Transmission Is Reliable and Temporally Precise

Heather J. Rose and Raju Metherate
Department of Neurobiology and Behavior, University of California, Irvine, California

Submitted 20 August 2004; accepted in final form 25 May 2005

Rose, Heather J. and Raju Metherate. Auditory thalamocortical transmission is reliable and temporally precise. *J Neurophysiol* 94: 2019–2030, 2005. First published May 31, 2005; doi:10.1152/jn.00860.2004. We have used the auditory thalamocortical slice to characterize thalamocortical transmission in primary auditory cortex (ACx) of the juvenile mouse. "Minimal" stimulation was used to activate medial geniculate neurons during whole cell recordings from regular-spiking (RS cells; mostly pyramidal) and fast-spiking (FS, putative inhibitory) neurons in ACx layers 3 and 4. Excitatory postsynaptic potentials (EPSPs) were considered monosynaptic (thalamocortical) if they met three criteria: low onset latency variability (jitter), little change in latency with increased stimulus intensity, and little change in latency during a high-frequency tetanus. Thalamocortical EPSPs were reliable (probability of postsynaptic responses to stimulation was ~1.0) as well as temporally precise (low jitter). Both RS and FS neurons received thalamocortical input, but EPSPs in FS cells had faster rise times, shorter latencies to peak amplitude, and shorter durations than EPSPs in RS cells. Thalamocortical EPSPs depressed during repetitive stimulation at rates (2–300 Hz) consistent with thalamic spike rates in vivo, but at stimulation rates ≥40 Hz, EPSPs also summed to activate *N*-methyl-D-aspartate receptors and trigger long-lasting polysynaptic activity. We conclude that thalamic inputs to excitatory and inhibitory neurons in ACx activate reliable and temporally precise monosynaptic EPSPs that in vivo may contribute to the precise timing of acoustic-evoked responses.

INTRODUCTION

Primary auditory cortex (ACx) neurons fire action potentials that reflect the onset of a stimulus, as well as frequency and intensity transitions within a complex stimulus, in a temporally precise manner (Eggermont 1995; Elhilali et al. 2004; Evans and Whitfield 1964; Heil and Irvine 1997; Phillips and Hall 1990). Spikes in ACx can be as tightly locked to the onset of a sound as spikes in cochlear nerve fibers, with trial-to-trial variability in spike latency, expressed as jitter (SD of latency), in the range of 0.1–10 ms (typically <1–2 ms) (Heil and Irvine 1997; Phillips and Hall 1990; reviewed by Phillips 1998). Similarly, spike responses to spectrotemporal transitions within complex stimuli often have <10-ms jitter (Elhilali et al. 2004). It seems therefore that precise spike timing occurs throughout the ascending auditory system, and even in ACx reflects the temporal fine structure of stimuli (Eggermont 1995; Elhilali et al. 2004). Notably, psychoacoustic studies show that animals with ACx lesions lose the ability to detect short gaps in tones (Buchtel and Stewart 1989; Ison et al. 1991; Kelly et al. 1996) and humans with ACx lesions poorly discriminate speech transitions in the milliseconds to tens-of-milliseconds range (Phillips and Farmer 1990). Thus the encoding of stimulus fine structure by ACx neurons may underlie perception of those features.

The maintenance of precise spike timing from cochlear nerve to ACx—four or more synapses away—likely requires specialized synaptic mechanisms, because jitter in synaptic onset latency typically increases with the number of synapses in a polysynaptic chain (Berry and Pentreath 1976). Synaptic specializations that preserve timing information are exemplified by calyceal synapses in the auditory brain stem (reviewed in Oertel 1999; Trussell 1999). Calyceal terminals generate postsynaptic currents many times larger than necessary to trigger a spike, thus reducing the jitter in latency to spike threshold. Postsynaptic specializations at these synapses include rapidly desensitizing neurotransmitter receptors and fast outward rectification (K^+ currents), both of which greatly limit the time window for spike generation. The combined effect of these specializations is to produce a synapse that is exceptionally secure in that each presynaptic action potential results in a reliable and precisely timed postsynaptic response (although not necessarily an action potential; Kopp-Scheinpflug et al. 2002).

Although there is no evidence for calyceal synapses in the auditory forebrain (Huang and Winer 2000; Winer 1992), the precision of spike timing in ACx suggests that synaptic mechanisms to preserve temporal information exist at each level of the auditory system, such as mechanisms that allow detection of convergent synaptic inputs. Evidence that synaptic jitter is low throughout the auditory "labeled line," at least for a subset of neurons, includes the remarkable observation that timing differences between the response onset to low and high-frequency stimuli in the cochlea (on the order of 0.5 ms/octave, because of travel time along the basilar membrane; Robles and Ruggero 2001) are preserved at the level of ACx (Kaur et al. 2004; Mendelson et al. 1997). ACx may employ cellular mechanisms similar to those described above. For example, ACx neurons with apparent strong rectification that fire only one to two spikes at very short latency in response to depolarizing current have been described (Metherate and Aramakis 1999). Furthermore, evidence from somatosensory cortex suggests that the efficacy of thalamocortical synapses is several times higher than that of intracortical synapses (i.e., more release sites and higher release probability; Gil et al. 1999). Similarly, thalamocortical synapses are structurally larger than intracortical synapses (Ahmed et al. 1994; Kharazia and Weinberg 1994). Finally, precise temporal integration of excitatory and inhibitory postsynaptic potentials (EPSPs and IPSPs, respectively) could also regulate the timing of acoustic-evoked spikes (Tan et al. 2004; Wehr and Zador 2003; Zhang et al. 2003). For the most part, however, the properties of identified synapses in ACx have not been examined.

Address for reprint requests and other correspondence: R. Metherate, Dept. of Neurobiology and Behavior, Univ. of California, Irvine, 2205 McGaugh Hall, Irvine, CA 92697-4550 (E-mail: rmethera@uci.edu).

The costs of publication of this article were defrayed in part by the payment of page charges. The article must therefore be hereby marked "*advertisement*" in accordance with 18 U.S.C. Section 1734 solely to indicate this fact.

In this study, we used the auditory thalamocortical slice (Cruikshank et al. 2002) to examine thalamocortical synapses in cortical layers 3 and 4, the major input layers of primary ACx (Caviness and Frost 1980; Romanski and LeDoux 1993; Winer 1992). First, we identified neurons in layers 3–4 as potentially inhibitory or excitatory based on their intrinsic membrane properties [fast spiking (FS) or regular spiking (RS), respectively] and morphology (determined subsequently in a subset of biocytin-filled neurons; Kawaguchi and Kubota 1997; McCormick et al. 1985). We used three criteria to identify monosynaptic thalamocortical EPSPs: *1*) low jitter of onset latency with "minimal"(single axon) stimulation, *2*) little change in onset latency with increased stimulus intensity, and *3*) little change in onset latency during a high-frequency tetanus. Finally, we determined how thalamocortical synapses respond to physiological rates of thalamic stimulation (2–300 Hz; Massaux et al. 2004). The results indicate that monosynaptic EPSPs exhibit little latency jitter and that monosynaptic EPSPs in FS (inhibitory) neurons have a faster time-course than those in RS neurons. Thalamocortical EPSPs depress with repetitive stimulation at 2–300 Hz, but nevertheless can sum at frequencies ≥40 Hz to trigger long-latency, polysynaptic activity. These findings suggest complementary roles for secure thalamocortical synapses and feed-forward IPSPs in generating precisely timed acoustic-evoked spikes in primary ACx.

METHODS

Thalamocortical slice preparation and maintenance

Auditory thalamocortical brain slices were prepared from 14- to 16-day FVB mice (Charles River), as described in detail in Cruikshank et al. (2002). After halothane anesthesia, the animal was decapitated, and the brain was quickly removed. The brain was submerged in cold artificial cerebral spinal fluid (ACSF) containing (in mM) 125.0 NaCl, 2.5 KCl, 25.0 $NaHCO_3$, 1.25 KH_2PO_4, 1.2 $MgSO_4$, 2.0 $CaCl_2$, and 10.0 dextrose, bubbled with 95% O_2-5% CO_2, pH 7.4. The brain was blocked, and 500-μm-thick near horizontal sections from the left hemisphere were obtained with a vibroslice (Leica VT 1000S). Sections were cut beginning with the ventral surface of the brain; the primary thalamocortical slice was visually identified based on local structure shape and size. One slice was saved per animal. The slices were placed in a room temperature holding chamber with oxygenated ACSF for ≥30 min before use. The slices were transferred to and submerged in a recording chamber where they were perfused with oxygenated ACSF at room temperature. The recording chamber was attached to a fixed stage of an upright microscope (Zeiss Axioscope), and neurons were visualized using infrared differential interference contrast (IR-DIC) optics with a video camera (Hamamatsu) and monitor.

Electrophysiological stimulation and recording

Pipettes for whole cell recording were pulled on a horizontal micropipette puller (P-97, Sutter Instrument) from filamented capillary glass and filled with (in mM) 130 $KMeSO_3$, 10 NaCl, 2 Mg-ATP, 0.5 Na-GTP, 10 HEPES, and 1.6 EGTA. The pH was adjusted to 7.2 and osmolarity to 295 mosmol/kg. Electrode resistance was 4–8 MΩ. Current-clamp recordings were obtained using an intracellular amplifier (Axoclamp 2B, Axon Instruments). A seal of 6 GΩ or greater was obtained, and the series resistance on rupturing the cell membrane was 8–40 MΩ. Series resistance was compensated using a bridge balance and adjusted as needed during recording. Voltages were not adjusted to compensate for the liquid junction potential (~10 mV).

Either the ventral division of the medial geniculate nucleus (MGv) or the initial portion of the thalamocortical pathway was stimulated using a programmable pulse generator (Master-8) and a constant current stimulus isolation unit (Axon Instruments). A bipolar stimulating electrode (~1 MOhm, 115 μm between poles, FHC) delivered monophasic stimulus pulses (5–140 μA; 200 μs). Stimulus generation and data collection were software controlled (AxoGraph, Axon Instruments), and data were stored on computer (PowerMac, Apple Computer). Data were digitized at 10 kHz.

Histology and pharmacological agents

Biocytin hydrochloride (1%, Sigma) was dissolved in the pipette solution (final concentration 0.5%) for some recordings. On completion of recording, slices with biocytin-filled cells were transferred to 4% paraformaldehyde for 48 h and to 0.1 M phosphate buffer until processing (up to 2 wk). Tissue was processed for biocytin as previously described (Metherate and Cruikshank 1999), and cells were viewed on a light microscope.

The contribution of *N*-methyl-D-aspartate (NMDA) receptors was studied using the antagonist (±)-2-amino-5-phosphono-valeric acid (APV; Sigma). In experiments designed to reduce polysynaptic activity, ACSF with increased divalent cation concentrations was used. This is referred to as high-divalent ACSF in the text. High-divalent ACSF contained (in mM) 115 NaCl, 2.5 KCl, 25.0 $NaHCO_3$, 4.2 $MgCl_2$, 7.0 $CaCl_2$, and 10.0 dextrose. Besides the increased magnesium and calcium concentrations, phosphates and sulfates were left out of the high-divalent ACSF to reduce calcium precipitation (see Crepel and Ben-Ari 1996; Cruikshank et al. 2002; Luhmann and Prince 1990).

Intrinsic properties

Input resistance was determined by measuring the voltage change in response to a small (−0.05 nA) hyperpolarizing current pulse; the time constant of the membrane was measured by fitting a first-order exponential function to the initial voltage curve in response to the same current pulse. Action potential threshold was measured at the point from which the rapidly rising phase of the spike began. Spike amplitude was measured from threshold, and spike width was measured at half-height.

The steady-state firing rate was measured from the number of spikes during the last 400 ms of a 700-ms depolarizing current pulse (+0.15 nA) that was well above threshold but not necessarily maximal. Spike frequency adaptation was measured in response to the lowest amplitude current pulse that resulted in firing throughout the pulse. Adaptation was calculated as the ratio of the interspike interval between the first and second spikes divided by the average interspike interval of the last four spikes. A value of one indicated no adaptation, whereas lesser values indicated adaptation.

Synaptic properties

For minimal stimulation, stimulus intensity was changed in small steps until an intensity value was reached that resulted in both responses and failures. The response to higher and lower intensities was also tested (steps as small as 0.5 μA when threshold was very low, and ≤20 μA for larger threshold values). At threshold intensity, 25–35 trials were collected; generally fewer were collected at the neighboring intensities.

To differentiate between responses, failures, and spontaneous events at minimal stimulation, Event Detection software (Axograph, Axon Instruments) was used to form a template based on the average of several clear responses with matching EPSP shape. Threshold detection was set at twice the SD of the template; EPSPs that fit the template were accepted as stimulus induced responses if the individual onset latency was within 4 ms of the average onset latency. After

event detection by the software, traces were visually inspected to add or remove events that had been categorized improperly. For example, an EPSP with a spontaneous event just before response onset or on the falling phase of the EPSP would sometimes be improperly chosen or discarded by the program. Trials categorized as failures were averaged; visual inspection of these averaged traces confirmed that there was, in fact, no synaptic response. A clear difference between responses and failures was required on overlaying all traces (i.e., all responses had to rise above the background noise). Because of this criterion, very small events may have been missed, and cells whose EPSPs displayed a continuous range of amplitudes between baseline noise and the largest EPSP peak would have been excluded. Responses at higher intensities were also required to retain the same shape, but with decreased probability of failure, for the threshold response to be considered likely to result from activation of a single axon and to be included in analysis.

Several parameters of the minimal stimulation-evoked EPSPs were measured. To determine the variability of EPSP amplitude in an individual cell, the baseline was set to zero between the stimulus artifact and response onset, and amplitude was measured over a 1-ms window at the peak of the EPSP, and the SD was calculated. The SD of baseline noise was calculated over a 1-ms window 5–15 ms before the region where baseline had been set to zero (the exact measurement region preceded the baseline region by the same latency which the peak amplitude followed the baseline region). The amplitude of all individual traces during this window was recorded and the SD of the amplitude was calculated. The SD of EPSP amplitude was corrected for the noise SD (by taking the square root of the sum of the squared SDs) and this noise-corrected amplitude SD is reported. Onset latencies of individual EPSPs were determined by fitting a first-order exponential curve to the initial EPSP slope, and the point at which this line crossed baseline was defined as the onset of the EPSP. Response onset latencies were analyzed for each cell to determine the range of values (longest onset latency minus the shortest) and SD.

All EPSPs in response to minimal stimulation were averaged (excluding failures), and rise time (20–80% peak amplitude), EPSP width at half-peak, and latency to peak were measured. After minimal stimulation, stimulation intensity was increased to elicit a clear and consistent response to each stimulus (~35% increase in intensity). Characteristics of average EPSPs in response to a suprathreshold stimulus were measured in the same manner as described for minimal stimulation. Suprathreshold EPSPs in response to a single stimulus are the average of 10–12 trials, with 8–10 s between trials.

The response to thalamocortical stimulation at varying frequencies was also recorded. Responses to frequency trains are averages of five to seven traces with 12 s between trials. The onset latency of individual EPSPs was measured as described above, with the exception that in cases where individual EPSPs were riding on a depolarized envelope, the onset was defined as the point at which the fitted curve crossed the decaying voltage from the preceding EPSPs. Also, individual EPSP amplitudes were measured from the membrane potential at response onset to the peak of the EPSP. Maximum depolarization was measured from baseline to the greatest depolarization reached during the trace; this usually occurred during the stimulus train or within 500 ms after the last stimulus pulse (1.5 s of activity were collected during 40-Hz tetani, the response always peaked well before the end of the collection period).

Data are presented as the mean ± SE. Statistical analysis was performed using software (SPSS 11.0 for Mac). Student's *t*-test (independent samples and paired samples) were used to compare two means, and a repeated-measures ANOVA was used to compare multiple values from one cell. For analyses, $P < 0.05$ was considered significant.

RESULTS

We used the auditory thalamocortical slice to examine thalamocortical synapses in layers 3 and 4 of primary ACx. We first identified neurons in layers 3–4 as RS or FS (likely excitatory or inhibitory, respectively) cells based on intrinsic membrane properties (and, in a few cases, morphology). We used three tests to identify monosynaptic EPSPs, and in doing so, characterized thalamocortical EPSPs. Finally, we determined how thalamocortical synapses respond to physiological rates of thalamic stimulation.

Stable whole cell recordings were obtained from 86 neurons in 37 thalamocortical slices. Cell depths ranged from 23 to 45% of the overall cortical depth, consistent with a location in layers 3 and 4 (Frost and Caviness 1980; Heumann et al. 1977).

RS and FS neurons in ACx layers 3–4

Neurons were categorized as RS or FS based on spike shape and the pattern of spike firing in response to a depolarizing current pulse (McCormick et al. 1985). Sixty-six cells (77%) were clearly RS, and 14 cells (16%) were FS (Fig. 1). FS cells are clearly differentiated from RS cells by their narrow spike width, fast spike afterhyperpolarization (AHP), fast membrane time constant, high steady-state firing rate, and little or no spike adaptation (Table 1). Although RS cells are sometimes categorized as adapting or nonadapting (Agmon and Connors 1992), we observed a continuum of adaptation rates (Fig. 1*D*). RS cells with little adaptation were distinguished from FS cells by other criteria, primarily spike width (Fig. 1*D*).

Six cells could not be clearly categorized as RS or FS. Three of these cells were similar to low-threshold spiking (LTS) cells, with a firing rate between RS and FS cells, complex AHPs and afterdepolarizations, and a last AHP at a more depolarized level than the first AHP (Beierlein et al. 2003). The other three cells each had a unique combination of FS, RS, and LTS intrinsic properties. Because these six cells could not be clearly categorized or were rare (in the case of LTS cells), they were not included in further analysis.

After initial recordings, it became clear that the recording sample was severely biased toward RS cells. Because one of the goals of the study was to determine if RS and FS cells process thalamocortical input differently, an attempt was made to target additional FS cells. However, although FS cells with their large oblong shape were easily identified visually (Beierlein and Connors 2002), they were difficult to find in layers 3–4, and the final percentage of FS cells remained low (16%). This was not caused by bias in our ability to successfully record from FS cells—the rate of successful recording after establishment of a GΩ seal was very high for both RS and FS cells. It seems that FS cells are sparse in layers 3 and 4 of primary ACx.

During some recordings, biocytin was included in the whole cell solution, and 10 physiologically identified cells were at least partially recovered. Of seven RS cells recovered, six were clearly pyramidal with spiny apical and basal dendrites. One RS neuron was a nonpyramidal multipolar cell with an axon that projected toward the white matter; spines were thinner and more difficult to detect than those on pyramidal neurons. Two FS cells were partially recovered; in both cases, the soma was not adequately recovered, but the cells had nonpyramidal dendritic morphology and axons projecting horizontally in the upper layers. One cell tentatively categorized as LTS also was recovered; this cell was bipolar with vertically oriented, aspiny processes. One group of dendrites branched in the upper layers

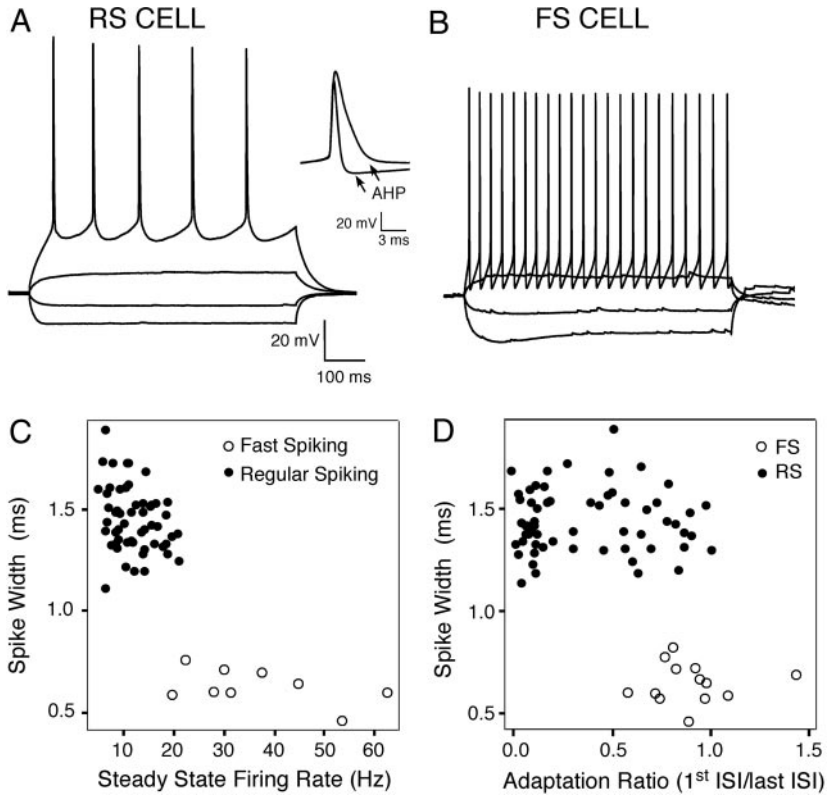

FIG. 1. Features of regular spiking (RS) and fast spiking (FS) cells in middle layers of primary auditory cortex (ACx). Current injection in both examples: −0.15, −0.05, +0.05, and +0.15 nA. *A*: RS neuron has broad spikes (*inset*: 1st spike for each example cell), shallow afterhyperpolarizing potential (AHP), and low steady-state firing rate; resting membrane potential (RMP) = −77 mV. *B*: FS neuron has narrow spike, strong AHP, and high firing rate; RMP = −63 mV. *C*: scatterplot of firing rate vs. spike width shows clear separation of RS and FS cells. *D*: FS and RS cells cannot be distinguished by degree of adaptation.

and reached the pia, whereas the lower group of dendrites projected toward the white matter ending near the border of layers 5 and 6. Several axonal branches projected toward the white matter. Thus the morphological data suggest that most (6/7) biocytin-filled RS cells were pyramidal and both FS cells were nonpyramidal.

Minimal stimulation of thalamocortical axons

After the characterization of intrinsic properties, cells were activated by thalamic stimulation either of the MGv proper or of the initial portion of the thalamocortical pathway. Stimulation was at a minimal intensity (~50% failure rate) with the intent of activating a single thalamocortical input (Isaac et al. 1997; Stevens and Wang 1995). The average intensity for minimal stimulation was 41.73 ± 3.09 μA (range, 5–120 μA). A minimal stimulation-evoked EPSP was considered caused by stimulation of a single axon if it met several criteria: a clear difference between successful responses and failures (all-or-none response) and an increased success rate with increased stimulus intensity that occurred without change in EPSP amplitude or shape (Fig. 2). In response to minimal stimulation, trial-to-trial variation in EPSP amplitudes could be small (Fig. 2*A*) or larger (Fig. 2*C*), but EPSPs with more variable amplitudes nonetheless displayed a consistent shape (apparent on normalization of amplitudes; Fig. 2*C*) and a clear distinction between events and failures. An increase in amplitude with increased stimulus intensity (data not shown) was taken as evidence that additional axons had been recruited. In practice, EPSPs were considered minimal stimulation-evoked if the failure rate decreased without change in EPSP shape with small changes (1–5 μA) in stimulus intensity. In a few instances stimuli were delivered over a broader range of intensities, and in most (4/5) of these cases, the highest stimulus intensities that still met the criterion of no change in EPSP shape resulted in no failures (i.e., success probability ~1.0; Fig. 2, *A–C*). These data suggest that cortical responses to stimulation of single thalamocortical neurons are highly reliable.

Of the original 80 RS and FS cells, 47 met the criteria for having a stable minimal stimulation-evoked response (37 RS and 10 FS cells). These cells were subjected to further tests to identify monosynaptic thalamocortical responses.

TABLE 1. *Intrinsic membrane properties of layer 3–4 RS and FS cells*

	RS	FS
Membrane potential, mV*	−74.3 ± 0.64	−69.7 ± 1.00
Input resistance, MΩ	204.4 ± 7.79	208.9 ± 23.24
Membrane time constant, ms*	20.0 ± 0.92	13.6 ± 1.40
Spike threshold, mV	42.6 ± 0.49	42.3 ± 1.27
Spike amplitude, mV*	84.5 ± 0.54	71.4 ± 1.86
Spike width, ms*†	1.43 ± 0.02	0.64 ± 0.03
Steady state firing rate, Hz*	12.4 ± 0.56	36.9 ± 4.85
Adaptation, 1st ISI/last ISI*	0.37 ± 0.04	0.92 ± 0.06

Values are mean ± SE *$P < 0.01$ comparing RS and FS cell means. †At half-amplitude. $N = 58–66$ RS cells and 9–14 FS cells. RS, regular spiking; FS, fast spiking.

Criteria for identifying monosynaptic EPSPs

Three additional physiological criteria (beyond having a minimal stimulation-evoked EPSP) were used to identify monosynaptic responses. The first criterion was based on the variability of onset latency (jitter) for the minimal stimulation-evoked response. Variability in onset latency was estimated from the range between the longest and shortest onset latency

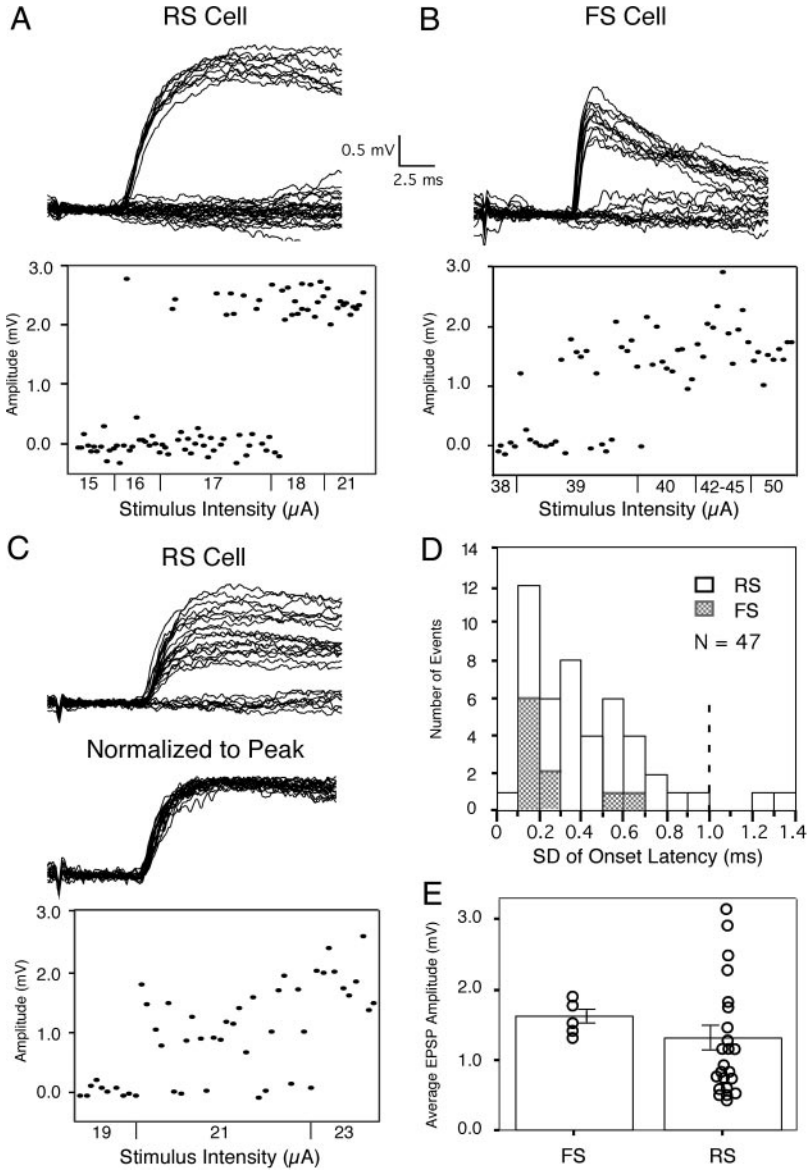

FIG. 2. Minimal stimulation-evoked excitatory postsynaptic potentials (EPSPs) in RS and FS cells. *A–C*: 3 examples that eventually were classified as presumed monosynaptic EPSPs. Voltage and time scale applies to all 3 examples. Scatterplot below each set of traces shows amplitudes for individual EPSPs and failures at threshold and neighboring stimulus intensities. Note in *C* that response amplitude is variable; however, a clear gap is visible between responses and failures and normalizing EPSP amplitudes reveals a consistent shape and onset slope. (RMP: *A*, −64 mV; *B*, −70 mV; *C*, −73 mV). *D*: distribution of onset latency SD (jitter) for all minimal stimulation-evoked EPSPs. Dashed line indicates 1-ms threshold for identifying potentially monosynaptic EPSPs. *E*: minimal stimulation-evoked EPSPs eventually classified as monosynaptic (see Figs. 3 and 4) had amplitudes that did not differ between RS cells ($n = 23$) and FS cells ($n = 5$).

(stimulation rate ~0.1 Hz; Fig. 2), and expressed as the SD (jitter) of onset latency. Dual intracellular recordings of synaptically connected cortical neurons have shown that EPSP onset latencies from single presynaptic action potentials can vary as much as 3 ms (Feldmeyer et al. 1999; Markram et al. 1997; Stern et al. 1992). In this study, an onset latency range of 3 ms corresponded approximately to a 1 ms SD. Therefore we considered that monosynaptic responses should have an onset latency SD of 1 ms or less. Minimal stimulation-evoked EPSPs in 45 of 47 cells met this criterion (Fig. 2*D*), indicating that nearly all layer 3–4 cells had low jitter responses to thalamic stimulation.

The second criterion for a monosynaptic response was that onset latency should not change with increased stimulus intensity. (If, for example, the EPSP at minimal intensity was disynaptic, a decrease in onset latency could occur if a higher stimulus intensity activated an axon projecting directly to the cell.) Stimulus intensity was increased above the minimal level by ~35% (referred to as suprathreshold stimulus intensity). The average onset latency in response to the suprathreshold stimulus was compared with the average onset latency of EPSPs (excluding failures) at the minimal intensity (Fig. 3*A*). With an estimate of synaptic delay of 0.3–0.5 ms (Berry and Pentreath 1976; Lin and Faber 2002) and EPSP rise times of 0.5–5.5 ms (mean of 2.12 ± 0.12 ms, 20–80% rise time from 47 minimal stimulation EPSPs), one intercalated neuron could cause a 0.8- to 6.0-ms difference in onset latency from a monosynaptic connection. Additionally, in the somatosensory thalamocortical system, disynaptic IPSPs have been observed as early as 1 ms after the earliest EPSP onset latency (Agmon and Connors 1992). We therefore considered that monosynaptic responses should exhibit less than a 1-ms decrease in onset latency with increasing intensity. Of the 46 cells tested for this criterion, 39 had EPSPs that exhibited <1 ms change in onset latency after an increase in stimulus intensity (Fig. 3*B*). Notably, the change in onset latency for EPSPs that failed to meet this criterion was substantial, with an average value of 3.7 ± 0.8 ms.

The third criterion for a monosynaptic response was the stability of the EPSP onset latency during a 40-Hz tetanus,

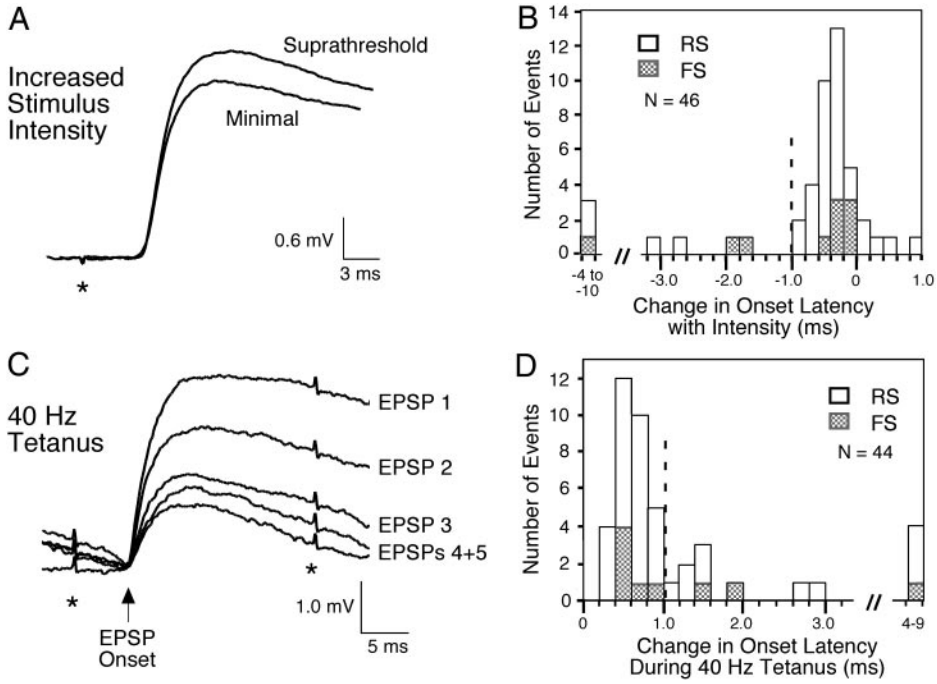

FIG. 3. Potentially monosynaptic, minimal stimulation-evoked EPSPs exhibited <1 ms changes in onset latency after an increase in stimulus intensity (*A* and *B*) and during a 40-Hz tetanus (*C* and *D*). Examples in *A* and *C* are both RS cells. *A*: suprathreshold-intensity stimulus (~35% increase from minimal intensity) in this cell decreased onset latency 0.1 ms. Traces are averages of 10–15 trials. *B*: change in onset latency after increase in stimulus intensity for all 46 cells tested. Values are onset latency at suprathreshold stimulation minus onset latency at minimal stimulus intensity (i.e., negative values indicate decreased latency with increased intensity). *C*: 40-Hz stimulus train at suprathreshold intensity in another cell produced a 0.4-ms change in onset latency. Traces show superimposed responses to 1st 5 stimuli (average of 4–5 trials each); baselines have been set to 0 at the latency of the earliest onset (arrow). Note that EPSPs after the 1st EPSP in a train often are riding on a depolarizing envelope (see Fig. 5). *D*: maximum change in onset latency during 1st 3–5 stimuli of the train for all cells. Asterisks in *A* and *C*, time of stimulus; dashed lines in *B* and *D*, 1-ms threshold for identifying potentially monosynaptic EPSPs.

because polysynaptic responses that depend on synaptic integration in intercalated neurons exhibit greater variability in onset latency during high-frequency stimulation (Berry and Pentreath 1976; Doyle and Andresen 2001). We measured the onset latency of the first three to five stimuli in the train (Fig. 3*C*; each measure is an average of 5–7 trials, performed at suprathreshold intensity). The latency of the EPSP with the shortest onset latency was subtracted from the EPSP with the longest onset latency; this difference is reported as the amount of change in EPSP onset latency during a 40-Hz tetanus (Fig. 3*D*). Although the literature does not provide measures of jitter at cortical synapses during high-frequency stimulation, and the expected jitter is difficult to estimate, following the logic above (expected jitter in *average* latency at one synapse is <1 ms, and 1 intercalated neuron may add >1 ms to a polysynaptic response latency), we considered that monosynaptic responses should exhibit a 1 ms or less change in average onset latency during a 40-Hz tetanus. Of the 44 cells tested, 31 cells met this criterion (Fig. 3*D*).

To be categorized as "presumed monosynaptic," an EPSP had to meet all criteria for which it was tested. Every EPSP was tested for at least two of the three criteria described above, and most (44 of 47) were tested for all three. Using this approach, EPSPs in 28 of 47 (60%) cells tested were presumed monosynaptic. Figure 4 shows the results for the 44 cases in which all three criteria were tested. To reiterate, presumed monosynaptic EPSPs exhibited *1*) <1-ms SD latency, *2*) <1-ms change in latency during a tetanus (EPSPs meeting these 2 criteria fall within the dashed lines in Fig. 4), and *3*) <1-ms decreased latency at suprathreshold intensity (EPSPs meeting this criterion are plotted as circles). It is interesting to note that in 10 of 14 instances where a cell missed the monosynaptic cutoff in

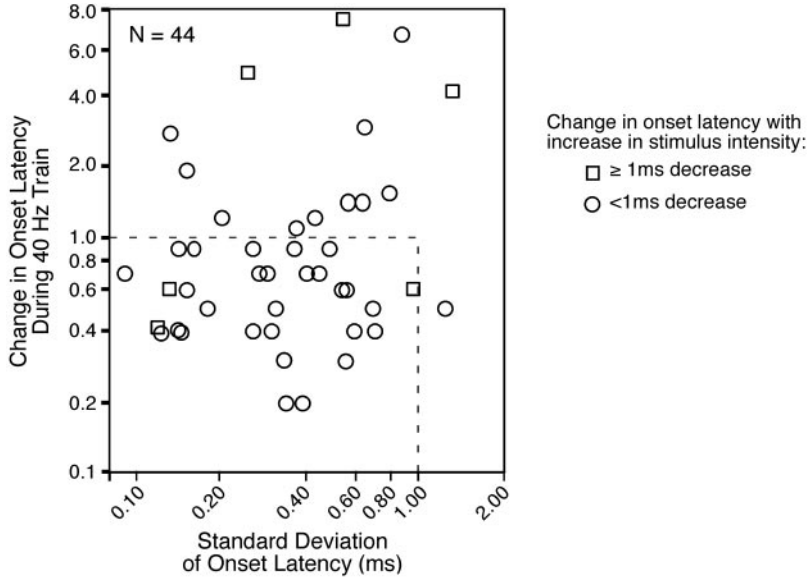

FIG. 4. Results for 44 neurons administered all 3 latency-based tests for monosynaptic thalamocortical EPSPs. Presumed monosynaptic EPSPs exhibited <1-ms jitter (SD of onset latency) during minimal stimulation, <1-ms change in onset latency with an increase in stimulus intensity, and <1-ms change in onset latency during a 40-Hz tetanus. EPSPs indicated by circles within the dashed lines met all 3 criteria and are categorized as presumed monosynaptic.

only one category, that category was latency change during a 40-Hz train; these same cells tended to have low jitter at minimal intensity and little change in latency at increased intensity. Similarly, whereas nearly all cells exhibited EPSPs with <1-ms jitter, 13 of these failed to meet one of the other two criteria.

Monosynaptic thalamocortical EPSPs in RS and FS cells

We next compared minimal stimulation-evoked, presumed monosynaptic EPSPs in FS and RS cells. The examples in Fig. 2 are from cells that eventually were categorized as monosynaptic, and mean monosynaptic EPSP characteristics are in Table 2. In general, monosynaptic EPSPs in FS cells had faster rise times, shorter latencies to peak, and shorter durations than monosynaptic EPSPs in RS cells. Average EPSP amplitudes in both kinds of cells were similar, although RS cells had a broader range of amplitudes (Fig. 2*E*). The trial-to-trial variability in amplitude (SD of amplitude, corrected for baseline noise SD of 0.07 ± 0.01 mV, see METHODS) also was the same for FS and RS cells. At the suprathreshold intensity (35% increase from minimal) that may resemble physiological conditions more closely (i.e., with multiple thalamic inputs activated), there still was no difference between amplitudes in FS cells (1.48 ± 0.21 mV; $n = 5$) and RS cells (1.75 ± 0.29 mV; $n = 23$; unpaired *t*-test, $P = 0.68$). Latency to peak amplitude did not change with increased intensity (at minimal intensity, 13.71 ± 0.57 ms vs. suprathreshold intensity, 14.48 ± 0.87 ms; $n = 28$, $P = 0.22$). Thus thalamocortical EPSPs may activate FS cells faster than RS cells.

Thalamic-evoked feed-forward inhibition

To determine if thalamic stimulation activated disynaptic or polysynaptic IPSPs that could inhibit the monosynaptic EPSP (reducing, e.g., its peak amplitude or duration), the membrane potential was depolarized beyond the expected IPSP reversal potential (approximately −70 mV) in 17 cells (4 FS and 13 RS cells). The suprathreshold stimulus intensity was used (58.27 ± 4.88 μA). Although the cells were depolarized close to spike threshold (in 5 cells the monosynaptic EPSP elicited a spike), in only 1 of the 17 cells did an IPSP become apparent as an abrupt, short latency hyperpolarization. In that case, the IPSP onset closely followed that of the initial EPSP, and prevented the EPSP from reaching peak amplitude. While more careful analysis, including pharmacological tests, is needed to more fully characterize the role of inhibition in ACx, strong IPSPs were not observed at the relatively low stimulus intensities used in this study.

TABLE 2. *Minimal stimulation-evoked monosynaptic EPSPs*

	RS	FS
Average onset latency, ms	7.14 ± 0.35	7.38 ± 0.67
SD of individual onsets, ms	0.36 ± 0.0	0.21 ± 0.04
Amplitude, mV	1.27 ± 0.17	1.62 ± 0.11
SD of amplitude, mV	0.30 ± 0.03	0.50 ± 0.10
Rise time, 20–80%; ms*	2.27 ± 0.10	0.84 ± 0.14
Latency to peak amplitude, ms*†	14.58 ± 0.50	9.7 ± 1.05
Width, ms*	38.47 ± 2.40	14.5 ± 2.50

Values are mean ± SE. *$P < 0.01$ comparing RS and FS cell means. †From stimulus artifact. $N = 23$ RS cells and 5 FS cells. ESPS, excitatory postsynaptic potential; RS, regular spiking; FS, fast spiking.

Response of thalamocortical synapses to physiological stimulation rates

Our next objective was to determine how neurons with presumed monosynaptic EPSPs respond to physiological rates of thalamic activation. Stimulation patterns were based on published accounts of tone-evoked tonic and burst firing for thalamic neurons in vivo (Massaux et al. 2004): 7 stimuli at 2 Hz, 10 stimuli at 10 Hz, 10 stimuli at 40 Hz, 3 stimuli at 100 Hz, and 3 stimuli at 300 Hz (all stimuli at suprathreshold intensity). EPSP peak amplitudes following individual stimuli were measured from baseline before response onset to allow measurement of EPSPs riding on a depolarizing envelope (e.g., Fig. 5).

Presumed monosynaptic EPSPs tended to depress at all stimulus frequencies (Fig. 5). At 2 and 10 Hz, the average EPSP amplitude decreased significantly (repeated-measures ANOVA, $n = 7$ cells for 2 Hz, $P < 0.05$; $n = 8$ cells for 10 Hz, $P < 0.005$). At 40 Hz, EPSPs also depressed (repeated-measures ANOVA, $n = 8$ cells, $P < 0.005$), although the large depolarizing envelope normally elicited by the train precluded measuring EPSPs beyond the first 3–5. At 100 Hz, average EPSP amplitude progressively decreased, but the change was not significant (repeated-measures ANOVA, $n = 7$ cells, $P = 0.11$; however, see Fig. 6*A*). At 300 Hz, individual EPSPs could not be resolved but the net depolarization appeared to indicate EPSP depression (Fig. 5).

Figure 6*A* shows the average responses to tetanic stimuli for all frequencies tested, with amplitudes normalized to the first EPSP in the train. Note that although EPSPs tended to depress at all frequencies, higher frequency stimuli often also produced long-latency polysynaptic activity that resulted in greater maximum depolarization (Fig. 5C). For 10- and 40-Hz stimuli, the data are also reported separately for RS and FS cells (Fig. 6, *B* and *C*; at other frequencies, too few FS cells were available for analysis). Stimuli at 10 Hz depressed the EPSP in FS cells (Fig. 6*B*; comparing EPSP 1 to EPSP 2, $n = 3$, $P = 0.03$), but did not affect the second EPSP in RS cells ($n = 6$, $P = 0.24$). Oddly, a 40-Hz tetanus produced dissimilar effects: in RS cells, EPSP amplitude depressed from stimulus 1 to 2 (Fig. 6C; paired *t*-test, $n = 20$, $P = 0.001$), whereas in FS cells, the EPSP did not change ($n = 5$, $P = 0.70$). The interaction of stimulus frequency and cell type will require further study to understand fully.

High-frequency stimulation-induced polysynaptic activity

A robust, long-latency depolarization that outlasted the stimulus train was observed in almost all cells in response to stimulation at higher frequencies (e.g., Fig. 5*C*). To study this apparently polysynaptic activity, we did not limit the analysis to cells with presumed monosynaptic EPSPs. The long-latency depolarization was observed consistently in response to 40-Hz (10 pulses) stimuli (Fig. 5*C*) and occasionally in response to 10- (10 pulses) and 100-Hz (3 pulses) stimuli. To determine if the depolarization depended more on the number of stimuli delivered or the stimulus rate, we measured peak depolarization in response to stimulus trains at 10 (10 pulses), 40 (10 or

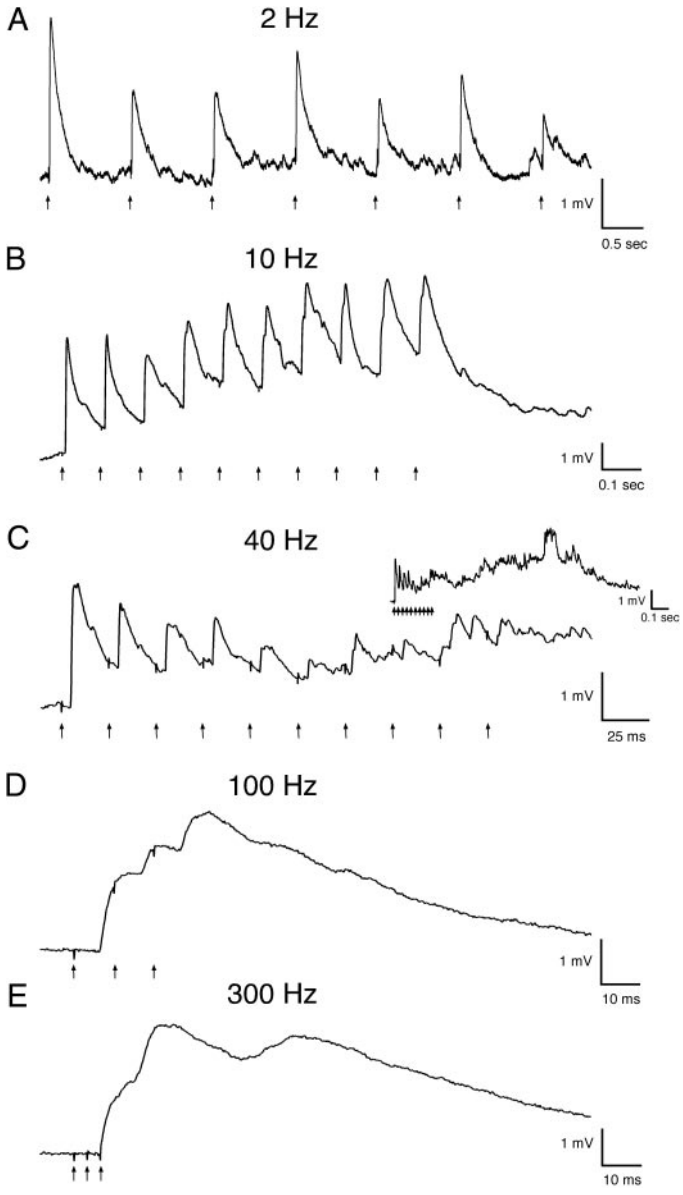

FIG. 5. Thalamocortical EPSPs depress in response to repetitive stimulation at physiological rates (2–300 Hz). A depolarizing envelope often developed at stimulation rates ≥10 Hz (*B*) and at 40 Hz continued well beyond the last stimulus pulse (*C, inset*). All cells are RS except FS cell in *C*. Arrows indicate stimulus time. RMP: −66 (*A*), −69 (*B*), −78 (*C*), −64 (*D*), and −67 mV (*E*).

3 pulses), and 100 Hz (10 pulses). Although 10- (10 pulses) and 40-Hz (3 pulses) trains occasionally elicited long-lasting depolarization, 40- (10 pulses) and 100-Hz (10 pulses) stimuli consistently elicited this response profile. The maximum depolarization reached was the same for 10 pulse trains at either 40 (4.5 ± 1.0 mV) or 100 Hz (4.6 ± 0.87 mV; paired *t*-test, $n = 6$, $P = 0.9$). Thus long-lasting intracortical depolarization can be produced when thalamic stimulation at sufficiently high frequencies (e.g., ~40 Hz or higher) is sufficiently prolonged (between 3 and 10 pulses).

Although three stimuli at 300 Hz generally did not elicit the long-lasting depolarization, this tetanus is of interest because the most common thalamic burst pattern in vivo consists of two to three spikes at 300 Hz (Massaux et al. 2004). The 300-Hz stimulus produced a larger depolarization (2.99 ± 0.37 mV) than that produced by a single thalamic stimulus (2.02 ± 0.34 mV; $n = 14$, $P < 0.005$). However, the 300-Hz tetanus was no more effective at depolarizing the cell than three stimuli at 40 or 100 Hz (40 Hz, 2.71 ± 0.37 mV; 100 Hz, 3.69 ± 0.78 mV; paired *t*-test, $n = 9$ or 11, $P > 0.05$).

Further studies of the long-lasting depolarization were conducted using a 40-Hz (10 pulses) tetanus. High divalent ACSF reversibly reduced the depolarization, confirming its polysynaptic nature (Fig. 7, *A and* B*; paired* t*-test,* n = *17,* P < *0.001). The NMDA receptor antagonist APV (25 μM) also reduced the depolarization reversibly (Fig. 7,* C *and* D*; paired* t*-test;* n = *15,* P < *0.001). Note that in seven cells (3 FS and 4 RS), APV had no significant effect on the amplitude, latency to peak, or width of presumed monosynaptic EPSPs in response to a single stimulus. Thus repetitive stimulation at higher frequencies may be required to activate the NMDA receptors involved in generating the long-lasting polysynaptic activity.*

DISCUSSION

We have used the auditory thalamocortical slice to examine thalamic-evoked synaptic potentials in cortical layers 3 and 4, the major input layers of primary ACx. The results show synaptic reliability and temporal precision at thalamocortical synapses. Presumed inhibitory (FS) and excitatory (RS) neurons in layers 3–4 both receive monosynaptic thalamocortical input, although FS neurons are relatively rare. Thalamocortical EPSPs in FS cells have faster rise times, shorter latencies to peak amplitude, and shorter durations than do thalamocortical EPSPs in RS cells. Thalamocortical EPSPs in both cell types depress during repetitive stimulation (2–300 Hz), yet higher stimulus frequencies (~40 Hz and greater) also elicit robust, long-lasting polysynaptic activity.

Identifying monosynaptic thalamocortical EPSPs

A main goal of this study was to determine the best method for isolating monosynaptic responses. Minimal (single axon) thalamic stimulation was used to improve the likelihood of activating only monosynaptic inputs. EPSPs were tested against three latency-based criteria. The first criterion was low onset latency jitter, which is commonly cited as evidence for a monosynaptic response (Berry and Pentreath 1976; Gil et al. 1999) and is more reliable than absolute onset latency (Doyle and Andresen 2001). Nearly all (96% of 47) minimal stimulation-evoked EPSPs met this criterion (jitter <1 ms), suggesting either that all minimal stimulation-evoked EPSPs are monosynaptic or that both monosynaptic and polysynaptic responses can have low jitter. In line with the latter possibility, in vivo recordings show that many ACx neurons exhibit jitter of <1–2 ms for tone-evoked spikes (Heil and Irvine 1997; Phillips and Hall 1990; reviewed in Phillips 1998).

The second criterion was little (<1 ms) decrease in onset latency with an increase in stimulus intensity. Most (85%) EPSPs also met this criterion, and the 15% that failed exceeded the criterion by a wide margin. For the EPSPs that failed, because we could not differentiate between initial, longer-latency responses being monosynaptic but slowly conducted (Beierlein and Connors 2002) versus being polysynaptic, all such responses were excluded from the "monosynaptic" pop-

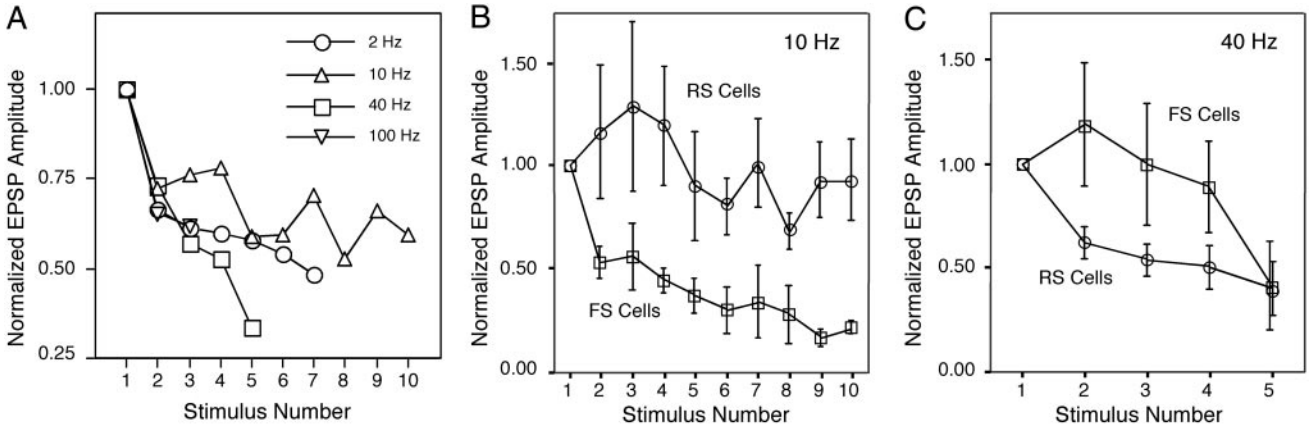

FIG. 6. Average thalamocortical responses generally depress during repetitive stimulation. *A*: data from RS and FS cells combined and amplitudes normalized to that of the 1st EPSP; error bars omitted for clarity. At 40 Hz, the 1st 3–5 responses were measured before EPSPs were generally obscured by the large fluctuating depolarization. Only 3 stimuli were delivered at 100 Hz. EPSP 2 is significantly smaller than EPSP 1 in response to all stimulus frequencies and EPSP 1 amplitude did not differ between groups. Mean values (in mV): 2 Hz EPSP 1 and 2: 1.22 ± 0.34, 0.81 ± 0.20, $n = 8$; 10 Hz EPSP 1 and 2: 1.52 ± 0.33, 1.09 ± 0.26, $n = 9$; 40 Hz EPSP 1 and 2: 1.65 ± 0.21, 1.21 ± 0.21, $n = 25$; 100 Hz, EPSP 1 and 2: 1.37 ± 0.50, 0.90 ± 0.29, $n = 7$. B: At 10 Hz, EPSPs in FS cells depressed (comparing 1st and 2nd EPSPs) whereas EPSPs in RS cells did not. *C*: at 40 Hz, EPSPs in RS cells depressed (comparing 1st and 2nd EPSPs), whereas EPSPs in FS cells did not. For *B* and *C*, mean values (in mV): 10 Hz FS cells: EPSP 1, 1.62 ± 0.12, EPSP 2, 0.90 ± 0.24, $n = 3$; 10 Hz RS cells: EPSP 1, 1.52 ± 0.57, EPSP 2, 1.27 ± 0.42, $n = 6$; 40 Hz FS cells: EPSP 1, 1.44 ± 0.20, EPSP 2, 1.63 ± 0.39, $n = 5$; 40 Hz RS cells: EPSP 1, 1.71 ± 0.25, EPSP 2, 1.11 ± 0.24, $n = 20$.

ulation. For the remaining EPSPs, it is possible that the ~35% increase in stimulus intensity was insufficient to reduce onset latency (e.g., by activating a more direct input to the cell). Thus the lack of change in latency is consistent with a monosynaptic response, but not conclusive.

The third criterion was little (<1 ms) change in onset latency during a 40-Hz tetanus. This seems to be the most stringent of the three latency-based criteria, in that it was met by only 70% of EPSPs. While it is possible that this criterion is too stringent and eliminated some monosynaptic EPSPs inappropriately, some EPSPs failed this criterion by a wide margin (≤9-ms change) and are unlikely to be monosynaptic. Clearly, no single test for a monosynaptic response is ideal, but combining the 40-Hz test with at least one other may be a reasonable and practical way to isolate monosynaptic thalamocortical EPSPs. Note that in other sensory cortices the presence of minimal stimulation-evoked EPSPs and/or low jitter alone are considered sufficient to identify thalamocortical EPSPs (Beierlein et al. 2003; Feldman et al. 1998; Gil et al. 1999). It remains to be determined whether the additional criteria required in the present study reflect differences in synaptic mechanisms among sensory cortices.

Functional connectivity between the MGv and layers 3 and 4 of ACx

While a major conclusion of this study is that thalamocortical synapses are temporally precise (low jitter), they also seem to be reliable (presynaptic stimuli nearly always produce

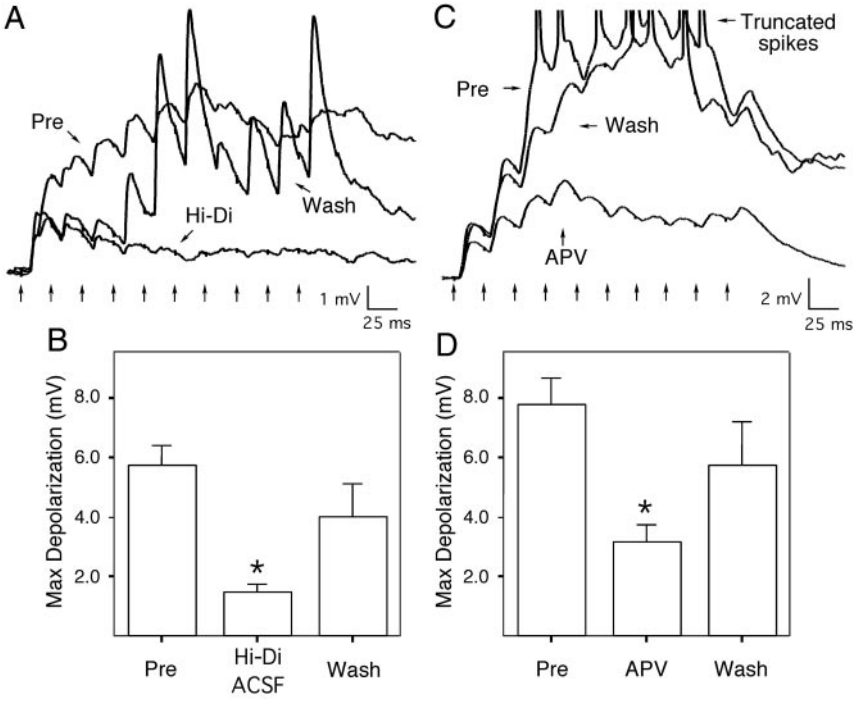

FIG. 7. Long-lasting activity in response to 40-Hz train is polysynaptic and involves NMDA receptors. *A*: high concentrations of divalent cations (Hi-Di; 7.0 mM Ca^{2+} and 4.2 mM Mg^{2+}) reversibly reduced the long-lasting depolarization. RMP, −72 mV. *B*: average effect of high divalent ACSF (predrug, 5.72 ± 0.67 mV, $n = 17$; Hi-Di 1.47 ± 0.28 mV, $n = 17$; wash, 4.02 ± 1.09 mV, $n = 10$). *C*: APV (25 μM) reversibly reduced the long-lasting depolarization. RMP, −66 mV. *D*: average effect of APV (control, 5.85 ± 0.41 mV, $n = 61$; APV 3.16 ± 0.57 mV, $n = 15$; wash, 5.73 ± 1.46, $n = 10$). Arrows, stimulus time; asterisk, $P < 0.05$ relative to control.

postsynaptic responses). Most data on minimal stimulation-evoked EPSPs were obtained over a narrow range of stimulus intensities that produced a mix of EPSPs and failures. In such cases, failures can result either from a failure of the stimulus to activate a thalamocortical neuron or from failure of an action potential invading the thalamocortical terminal to produce transmitter release. However, in a few cases, the stimulus was varied over a wider range of intensities. In most (4 of 5) of these cases, the highest-intensity single-axon stimulation resulted in no failures (Fig. 2). While the data are limited, they suggest that thalamic stimuli of sufficient intensity to activate thalamocortical neurons almost always produce postsynaptic responses (i.e., success probability near 1.0). This value is higher than estimates of success probability at many cortical synapses (e.g., 0.2–0.6 in CA1 hippocampus, Stevens and Wang 1995; release probability <0.2 in visual cortex layer 2/3, Volgushev et al. 2004). Data from the somatosensory system similarly suggest that thalamocortical terminals have 50% higher release probability and three times more release sites than intracortical synapses (Gil et al. 1999), although this relative measure depends on the intracortical synapse being tested (Silver et al. 2003). In any case, the data reinforce the notion that auditory thalamocortical transmission is highly secure.

Another goal of this study was to compare thalamocortical inputs to excitatory and inhibitory neurons, which we infer by examining RS and FS cells, respectively. Most RS cells are glutamate-containing (excitatory) pyramidal neurons, and FS cells are GABA-containing (inhibitory) interneurons (Kawaguchi and Kubota 1997; McCormick et al. 1985). However, some nonpyramidal, presumed inhibitory neurons exhibit RS patterns (Kawaguchi and Kubota 1996; Porter et al. 2001). Thus in this study, we have not identified all types of inhibitory neuron (only those that are FS), and some of our RS cells may be inhibitory. However, our general assumption that most RS cells are excitatory is supported by the fact that six of seven biocytin-filled RS cells were pyramidal, and all seven cells exhibited dendritic spines.

Monosynaptic thalamocortical EPSPs in FS cells exhibited faster rise times, shorter latencies to peak, and shorter durations than in RS cells. The fast time-course of FS cell EPSPs may mediate fast, feed-forward inhibition to reduce the spread of excitation in ACx, both temporally and spatially. Fast IPSPs may regulate spike timing by closing the window for spike generation and limiting the number of spikes in response to an auditory stimulus. Such a mechanism could contribute to the typical one to two spike "onset response" to auditory stimuli (Calford and Semple 1995; DeWeese et al. 2003; Evans and Whitfield 1964) and could play a role in regulating precise timing of spikes. However, note that the faster time course of thalamocortical EPSPs in FS cells was not associated with a larger amplitude, in contrast to data from the somatosensory thalamocortical slice (Beierlein et al. 2002; Gibson et al. 1999). Combined with the sparseness of FS cells in the middle layers of ACx, this may indicate a lesser role for thalamocortical feed-forward inhibition in auditory cortex than in other sensory cortices (Gibson et al. 1999; Gil and Amitai 1996; Krukowski and Miller 2001; Miller 2003; Porter et al. 2001). Notably, a thalamic stimulus-evoked IPSP was observed in only one cell in this study, and previously we observed that IPSPs evoked by thalamic stimuli are weaker than those evoked by intracortical stimuli (Cruikshank et al. 2002). Although cortical inhibition may not be fully developed at this age (Luhmann and Prince 1990), apparent IPSPs were observed during the polysynaptic activity elicited by high-frequency trains. These findings indicate that thalamic input may not activate inhibitory networks in ACx as strongly as do other inputs, though pharmacological studies, and studies using a wider range of stimulus intensities, are needed to fully investigate the role of inhibition in the auditory thalamocortical slice.

Dynamics of thalamocortical EPSPs during repetitive stimulation

Thalamocortical EPSPs tended to depress strongly during repetitive thalamic stimulation at 2–300 Hz. This process likely contributes to the poor ability of cortical neurons to follow repetitive acoustic stimuli (e.g., click trains) despite the much better performance of neurons in the MGv (Eggermont 1991, 1994). Our results are consistent with those from other thalamocortical systems in vivo (Fuentealba et al. 2004) and in vitro (Beierlein et al. 2002, 2003; Gibson et al. 1999; Gil et al. 1999), in which depression involves presynaptic mechanisms (Gil et al. 1999). A small subset of EPSPs did not depress (and some appeared to facilitate) over the course of several stimuli. It is possible that the few facilitating EPSPs arise not from thalamocortical inputs but from collaterals of antidromically activated corticothalamic neurons (Beierlein et al. 2002, 2003). Variable responses to repetitive stimulation might also involve developmental changes in release probability (Bolshakov and Siegelbaum 1995; Reyes and Sakmann 1999).

Tetanic thalamic stimulation resulted in long-latency polysynaptic activity that lasted several hundred milliseconds and was mediated at least partly by NMDA receptors. Similar NMDA receptor–dependent activity occurs in somatosensory cortex from thalamocortical activation of just a few layer 4 neurons; this activity is amplified in layer 4 before spreading to the upper layers (Beierlein et al. 2002). These data suggest that temporal summation of EPSPs may occur in a few critical layer 3–4 neurons at higher stimulus frequencies; the resulting depolarization enables the activation of NMDA receptors and triggers long-duration polysynaptic activity (Metherate and Cruikshank 1999). Data from thalamic recordings in the awake animal show tone-evoked responses comprise tonic firing at 40 Hz combined with bursts of $\leq$300 Hz (Massaux et al. 2004). Thus the thalamic stimulation rates in this study that were most effective in triggering polysynaptic activity resemble in vivo thalamic spike rates elicited by optimal tones.

Implications for mechanisms of auditory thalamocortical transmission

This study shows that thalamocortical EPSPs are reliable and temporally precise. These conclusions raise several questions about underlying mechanism. Secure monosynaptic EPSPs need not depend on highly specialized synaptic machinery such as at calyceal synapses (see Introduction), yet the high success probability at thalamocortical synapses likely requires high release probability at each thalamocortical release site as well as multiple release sites per thalamocortical axon. Additional mechanisms may contribute to the high temporal precision observed in this study.

Even if thalamocortical EPSPs have temporally precise onsets, an important question remains how such EPSPs produce precisely timed spikes (e.g., in response to acoustic stimulation; see Introduction). In this study, thalamic stimulus-evoked spikes were never observed, presumably due, at least in part, to the use of near-minimal stimulus intensities. (The presence of polysynaptic responses could result from minimal stimulation for the recorded neuron being suprathreshold for other neurons, thereby initiating polysynaptic activity.) At higher stimulus intensities, precise timing of spikes could be promoted by fast feed-forward inhibition that would prevent longer latency spiking, or by fast, outward (K^+) currents that serve the same function. Layer 4 neurons with fast, apparent membrane rectification that limits excitation to one spike have been observed previously in ACx (Metherate and Aramakis 1999) but are quite rare (<2% of 233 neurons) and were not observed in this study. Notably, imaging studies of somatosensory thalamocortical slices have shown that thalamic stimuli produce spikes in very few (<1%) layer 4 cells, yet subsequent electrophysiological recordings from these same neurons revealed unusually large minimal stimulation-evoked EPSPs (Beierlein et al. 2002). These layer 4 "gateway" neurons rapidly amplify thalamocortical inputs (note, however, that their spike latency was variable; Beierlein et al. 2002; see also Douglas and Martin 1991). Future studies designed to sample all cell types in layers 3 and 4 may help answer the question of how thalamic inputs are relayed in layers 3–4 of primary ACx.

ACKNOWLEDGMENTS

We thank R. Lazar for biocytin processing.

GRANTS

This work was supported by NIH Grants 5 F31 DC-05723 to H. J. Rose, R01 DC-02967, and R01 DA-12929.

REFERENCES

Agmon A and Connors BW. Correlation between intrinsic firing patterns and thalamocortical synaptic responses of neurons in mouse barrel cortex. *J Neurosci* 12: 319–329, 1992.

Ahmed B, Anderson JC, Douglas RJ, Martin KA, and Nelson JC. Polyneuronal innervation of spiny stellate neurons in cat visual cortex. *J Comp Neurol* 341: 39–49, 1994.

Beierlein M and Connors BW. Short-term dynamics of thalamocortical and intracortical synapses onto layer 6 neurons in neocortex. *J Neurophysiol* 88: 1924–1932, 2002.

Beierlein M, Fall CP, Rinzel J, and Yuste R. Thalamocortical bursts trigger recurrent activity in neocortical networks: layer 4 as a frequency-dependent gate. *J Neurosci* 22: 9885–9894, 2002.

Beierlein M, Gibson JR, and Connors BW. Two dynamically distinct inhibitory networks in layer 4 of the neocortex. *J Neurophysiol* 90: 2987–3000, 2003.

Berry MS and Pentreath VW. Criteria for distinguishing between monosynaptic and polysynaptic transmission. *Brain Res* 105: 1–20, 1976.

Bolshakov VY and Siegelbaum SA. Regulation of hippocampal transmitter release during development and long-term potentiation. *Science* 269: 1730–1734, 1995.

Buchtel HA and Stewart JD. Auditory agnosia: apperceptive or associative disorder? *Brain Lang* 37: 12–25, 1989.

Calford MB and Semple MN. Monaural inhibition in cat auditory cortex. *J Neurophysiol* 73: 1876–1891, 1995.

Caspary DM, Backoff PM, Finlayson PG, and Palombi PS. Inhibitory inputs modulate discharge rate within frequency receptive fields of anteroventral cochlear nucleus neurons. *J Neurophysiol* 72: 2124–2133, 1994.

Caviness VS Jr. and Frost DO. Tangential organization of thalamic projections to the neocortex in the mouse. *J Comp Neurol* 194: 335–367, 1980.

Crepel V and Ben-Ari Y. Intracellular injection of a Ca^{2+} chelator prevents generation of anoxic LTP. *J Neurophysiol* 75: 770–779, 1996.

Cruikshank SJ, Rose HJ, and Metherate R. Auditory thalamocortical synaptic transmission in vitro. *J Neurophysiol* 87: 361–384, 2002.

DeWeese MR, Wehr M, and Zador AM. Binary spiking in auditory cortex. *J Neurosci* 23: 7940–7949, 2003.

Douglas RJ and Martin KA. A functional microcircuit for cat visual cortex. *J Physiol* 440: 735–769, 1991.

Doyle MW and Andresen MC. Reliability of monosynaptic sensory transmission in brain stem neurons in vitro. *J Neurophysiol* 85: 2213–2223, 2001.

Eggermont JJ. Rate and synchronization measures of periodicity coding in cat primary auditory cortex. *Hear Res* 56: 153–167, 1991.

Eggermont JJ. Temporal modulation transfer functions for AM and FM stimuli in cat auditory cortex. Effects of carrier type, modulating waveform and intensity. *Hear Res* 74: 51–66, 1994.

Eggermont JJ. Representation of a voice onset time continuum in primary auditory cortex of the cat. *J Acoust Soc Am* 98: 911–920, 1995.

Elhilali M, Fritz JB, Klein DJ, Simon JZ, and Shamma SA. Dynamics of precise spike timing in primary auditory cortex. *J Neurosci* 24: 1159–1172, 2004.

Evans E and Whitfield IC. Classification of unit responses in the auditory cortex of the unanesthetized and unrestrained cat. *J Physiol* 171: 476–493, 1964.

Feldman DE, Nicoll RA, Malenka RC, and Isaac JT. Long-term depression at thalamocortical synapses in developing rat somatosensory cortex. *Neuron* 21: 347–357, 1998.

Feldmeyer D, Egger V, Lubke J, and Sakmann B. Reliable synaptic connections between pairs of excitatory layer 4 neurones within a single 'barrel' of developing rat somatosensory cortex. *J Physiol* 521: 169–190, 1999.

Frost DO and Caviness VS Jr. Radial organization of thalamic projections to the neocortex in the mouse. *J Comp Neurol* 194: 369–393, 1980.

Fuentealba P, Crochet S, Timofeev I, and Steriade M. Synaptic interactions between thalamic and cortical inputs onto cortical neurons in vivo. *J Neurophysiol* 91: 1990–1998, 2004.

Gibson JR, Beierlein M, and Connors BW. Two networks of electrically coupled inhibitory neurons in neocortex. *Nature* 402: 75–79, 1999.

Gil Z and Amitai Y. Properties of convergent thalamocortical and intracortical synaptic potentials in single neurons of neocortex. *J Neurosci* 16: 6567–6578, 1996.

Gil Z, Connors BW, and Amitai Y. Efficacy of thalamocortical and intracortical synaptic connections: quanta, innervation, and reliability. *Neuron* 23: 385–397, 1999.

Heil P and Irvine DR. First-spike timing of auditory-nerve fibers and comparison with auditory cortex. *J Neurophysiol* 78: 2438–2454, 1997.

Heumann D, Leuba G, and Rabinowicz T. Postnatal development of the mouse cerebral neocortex. II. Quantitative cytoarchitectonics of visual and auditory areas. *J Hirnforsch* 18: 483–500, 1977.

Huang CL and Winer JA. Auditory thalamocortical projections in the cat: laminar and areal patterns of input. *J Comp Neurol* 427: 302–331, 2000.

Isaac JT, Crair MC, Nicoll RA, and Malenka RC. Silent synapses during development of thalamocortical inputs. *Neuron* 18: 269–280, 1997.

Ison JR, O'Connor K, Bowen GP, and Bocirnea A. Temporal resolution of gaps in noise by the rat is lost with functional decortication. *Behav Neurosci* 105: 33–40, 1991.

Kaur S, Lazar R, and Metherate R. Intracortical pathways determine breadth of subthreshold frequency receptive fields in primary auditory cortex. *J Neurophysiol* 91: 2551–2567, 2004.

Kawaguchi Y and Kubota Y. Physiological and morphological identification of somatostatin- or vasoactive intestinal polypeptide-containing cells among GABAergic cell subtypes in rat frontal cortex. *J Neurosci* 16: 2701–2715, 1996.

Kawaguchi Y and Kubota Y. GABAergic cell subtypes and their synaptic connections in rat frontal cortex. *Cereb Cortex* 7: 476–486, 1997.

Kelly JB, Rooney BJ, and Phillips DP. Effects of bilateral auditory cortical lesions on gap-detection thresholds in the ferret (Mustela putorius). *Behav Neurosci* 110: 542–550, 1996.

Kharazia VN and Weinberg RJ. Glutamate in thalamic fibers terminating in layer IV of primary sensory cortex. *J Neurosci* 14: 6021–6032, 1994.

Kopp-Scheinpflug C, Dehmel S, Dorrscheidt GJ, and Rubsamen R. Interaction of excitation and inhibition in anteroventral cochlear nucleus neurons that receive large endbulb synaptic endings. *J Neurosci* 22: 11004–11018, 2002.

Krukowski AE and Miller KD. Thalamocortical NMDA conductances and intracortical inhibition can explain cortical temporal tuning. *Nat Neurosci* 4: 424–430, 2001.

Lin JW and Faber DS. Modulation of synaptic delay during synaptic plasticity. *Trends Neurosci* 25: 449–455, 2002.

Luhmann HJ and Prince DA. Transient expression of polysynaptic NMDA receptor-mediated activity during neocortical development. *Neurosci Lett* 111: 109–115, 1990.

Markram H, Lubke J, Frotscher M, Roth A, and Sakmann B. Physiology and anatomy of synaptic connections between thick tufted pyramidal neurones in the developing rat neocortex. *J Physiol* 500: 409–440, 1997.

Massaux A, Dutrieux G, Cotillon-Williams N, Manunta Y, and Edeline JM. Auditory thalamus bursts in anesthetized and non-anesthetized states: contribution to functional properties. *J Neurophysiol* 91: 2117–2134, 2004.

McCormick DA, Connors BW, Lighthall JW, and Prince DA. Comparative electrophysiology of pyramidal and sparsely spiny stellate neurons of the neocortex. *J Neurophysiol* 54: 782–806, 1985.

Mendelson JR, Schreiner CE, and Sutter ML. Functional topography of cat primary auditory cortex: response latencies. *J Comp Physiol [A]* 181: 615–633, 1997.

Metherate R and Aramakis VB. Intrinsic electrophysiology of neurons in thalamorecipient layers of developing rat auditory cortex. *Brain Res Dev Brain Res* 115: 131–144, 1999.

Metherate R and Cruikshank SJ. Thalamocortical inputs trigger a propagating envelope of gamma-band activity in auditory cortex in vitro. *Exp Brain Res* 126: 160–174, 1999.

Miller KD. Understanding layer 4 of the cortical circuit: a model based on cat V1. *Cereb Cortex* 13: 73–82, 2003.

Oertel D. The role of timing in the brain stem auditory nuclei of vertebrates. *Annu Rev Physiol* 61: 497–519, 1999.

Phillips DP. Sensory representations, the auditory cortex, and speech perception. *Sem Hear* 19: 319–331, 1998.

Phillips DP and Farmer ME. Acquired word deafness and the temporal grain of sound representation in the primary auditory cortex. *Behav Brain Res* 40: 85–94, 1990.

Phillips DP and Hall SE. Response timing constraints on the cortical representation of sound time structure. *J Acoust Soc Am* 88: 1403–1411, 1990.

Porter JT, Johnson CK, and Agmon A. Diverse types of interneurons generate thalamus-evoked feedforward inhibition in the mouse barrel cortex. *J Neurosci* 21: 2699–2710, 2001.

Reyes A and Sakmann B. Developmental switch in the short-term modification of unitary EPSPs evoked in layer 2/3 and layer 5 pyramidal neurons of rat neocortex. *J Neurosci* 19: 3827–3835, 1999.

Robles L and Ruggero MA. Mechanics of the mammalian cochlea. *Physiol Rev* 81: 1305–1352, 2001.

Romanski LM and LeDoux JE. Organization of rodent auditory cortex: anterograde transport of PHA-L from MGv to temporal neocortex. *Cereb Cortex* 3: 499–514, 1993.

Rose HJ and Metherate R. Thalamic stimulation largely elicits orthodromic, rather than antidromic, cortical activation in an auditory thalamocortical slice. *Neuroscience* 106: 331–340, 2001.

Silver RA, Lubke J, Sakmann B, and Feldmeyer D. High-probability uniquantal transmission at excitatory synapses in barrel cortex. *Science* 302: 1981–1984, 2003.

Stern P, Edwards FA, and Sakmann B. Fast and slow components of unitary EPSCs on stellate cells elicited by focal stimulation in slices of rat visual cortex. *J Physiol* 449: 247–278, 1992.

Stevens CF and Wang Y. Facilitation and depression at single central synapses. *Neuron* 14: 795–802, 1995.

Tan AY, Zhang LI, Merzenich MM, and Schreiner CE. Tone-evoked excitatory and inhibitory synaptic conductances of primary auditory cortex neurons. *J Neurophysiol* 92: 630–643, 2004.

Trussell LO. Synaptic mechanisms for coding timing in auditory neurons. *Annu Rev Physiol* 61: 477–496, 1999.

Volgushev M, Kudryashov I, Chistiakova M, Mukovski M, Niesmann J, and Eysel UT. Probability of transmitter release at neocortical synapses at different temperatures. *J Neurophysiol* 92: 212–220, 2004.

Wehr M and Zador AM. Balanced inhibition underlies tuning and sharpens spike timing in auditory cortex. *Nature* 426: 442–446, 2003.

Winer JA. The functional architecture of the medial geniculate body and primary auditory cortex. In: *The Mammalian Auditory Pathway: Neuroanatomy*, edited by Webster DB, Popper AN, and Fay RR. New York: Springer-Verlag, 1992, p. 222–409.

Zhang LI, Tan AY, Schreiner CE, and Merzenich MM. Topography and synaptic shaping of direction selectivity in primary auditory cortex. *Nature* 424: 201–205, 2003.